

Unusual Polybrominated Polypyrazolylborates and Their Copper(I) Complexes: Synthesis, Characterization, and Catalytic Activity

Glen P. A. Yap,[†] Fernando Jove,[†] Juan Urbano,[‡] Eleuterio Alvarez,[§] Swiatoslaw Trofimenko,^{*,†} M. Mar Díaz-Requejo,^{*,‡} and Pedro J. Pérez^{*,‡}

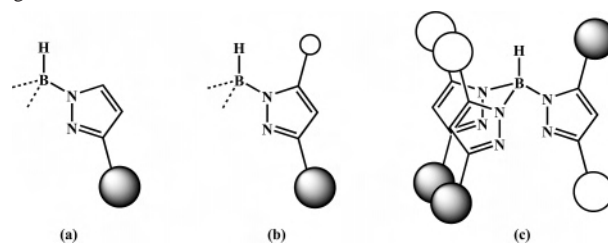
Department of Chemistry and Biochemistry, University of Delaware, Newark, Delaware 19716, Laboratorio de Catálisis Homogénea, Departamento de Química y Ciencia de los Materiales, Unidad Asociada al CSIC, Campus de El Carmen s/n, Universidad de Huelva, 21007-Huelva, Spain, and Instituto de Investigaciones Químicas, CSIC-Universidad de Sevilla, Avda. Américo Vespucio 49, 41092 Sevilla, Spain

Received September 10, 2006

Five new homoscorpionate ligands were prepared and structurally characterized as their Tl complexes, three of which, Tl[Tp^{Br,Ph,Br}] (1) (Tp = hydrotris(pyrazolyl)borate), Tl[Tp^{Br,ρ-Tol,Br}] (2), and Tl[Tp^{Br,ρ-ClPh,Br}] (3), are unique in being the first examples of an “atypical” B–N bond to the most sterically hindered pyrazole nitrogen. They contain bromine atoms on the central and outer carbons of the pyrazole ring, with all aryl substituents in the 5-position of the ligand, forming a protective pocket around the B–H bond. These complexes display a rather high B–H stretch frequency (above 2 600 cm⁻¹) in the IR region. Two other ligands, Tl[Tp^{ρ-ClPh,4Br}] (4) and Tl[Tp^{Ph,Me,Br}] (5), containing no outer bromine substituents, have normal B–N bonding to the least-hindered nitrogen. These new ligands have been employed to prepare the series of complexes Tp^xCu(NCMe) (6–10), for which X-ray studies of two of them (7 and 10) have shown that the atypical or normal geometry of the ligands is maintained when complexed to the copper center. The new complexes have also been tested as the catalysts in carbene and nitrene transfer reactions providing moderate to high yields in the expected products.

Introduction

One of the truisms in polypyrazolylborate chemistry has been that 3-substituted pyrazoles give rise to ligands in which the boron is bonded to the least-hindered nitrogen of the pyrazolyl ring, and the substituent winds up in the 3-position (Scheme 1a).¹ In the case of asymmetrically 3,5-disubstituted pyrazoles, boron is also bonded to the least-hindered nitrogen, so that the bulky substituent is again in the 3-position (Scheme 1b). When the 3- and 5-substituents are close in size, a mixture of isomers is obtained. Occasionally the ligand isolated has 3,3,5-substitution, that is, two substituents are in the 3-position and the other one in the 5-position, as was

Scheme 1. Possible Geometries for Unsymmetrically Substituted Tp^x Ligands

found in the case of hydrotris(3-mesitylpyrazol-1-yl)borate (Tp^{Ms}) and hydro[(bis(3-mesityl))(5-mesityl)](pyrazol-1-yl)borate (Tp^{Ms*}) (Scheme 1c).² The 3,3,5-substitution can also be obtained via rearrangement of a 3,3,3-ligand as, for instance, in the formation of octahedral L₂M complexes derived from Tp^{iPr}.³ It is so in the case of indazoles, where

* To whom correspondence should be addressed. E-mail address: trofimen@udel.edu (S.T.); perez@dqcm.uhu.es (P.J.P.); mmdiaz@dqcm.uhu.es (M.M.D.R.).

[†] University of Delaware.

[‡] Universidad de Huelva.

[§] CSIC-Universidad de Sevilla.

(1) (a) Trofimenko, S. *Chem. Rev.* **1993**, 93, 943–980. (b) *Scorpionates: The Coordination Chemistry of Polypyrazolylborate Ligands*; Imperial College Press: London, 1999.

(2) (a) Rheingold, A. L.; White, C. B.; Trofimenko, S. *Inorg. Chem.* **1993**, 32, 3471. (b) Silva, M.; Domingos, A.; Pires de Matos, A.; Marques, N.; Trofimenko, S. *J. Chem. Soc., Dalton Trans.* **2000**, 4628.

(3) Trofimenko, S.; Calabrese, J. C.; Domaille, P. J.; Thompson, J. S. *Inorg. Chem.* **1989**, 28, 1091.

a benzo ring is fused onto the pyrazole ring, such that the boron is bonded to the more-hindered nitrogen, as electronic effects override the steric ones.⁴ The only exception here is the case of 7-substituted indazoles, where boron is indeed bonded to the less-hindered nitrogen. Examples of Tp^x ligands where boron is bonded to the more-hindered nitrogen and all three bulky substituents are in the 5-position have not been found to date.

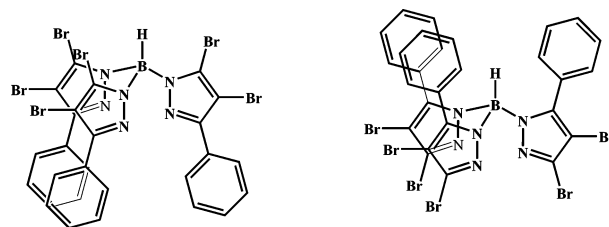
Earlier, we established that the copper(I) complex containing the $\text{HB}(3,4,5\text{-Br}_3\text{-pz})_3$ (pz = pyrazolyl) ligand (Tp^{Br_3}) is a very active catalyst for a number of reactions. These included C–H activation not only in various hydrocarbons^{5,6} but even in polyolefins,⁷ carbene insertion into –OH bonds,⁸ carbene addition to furans,⁹ or olefin aziridination.¹⁰ Activation of primary C–H bonds with a silver complex¹¹ and the alkane dehydrogenation with an Ir(I) complex¹² have also been reported. After these results, we decided to investigate related ligands in which one outer bromine is replaced by a bulky substituent, using 3-(Ar)-4,5-dibromopyrazoles as the starting materials. Much to our surprise, these ligands had all their aryl groups in the 5-position; that is, boron was bonded to the *more-hindered* nitrogen. We report herein the syntheses and characterization of this new family of trispyrazolylborate ligands, as well as their copper(I) complexes, that have also been tested as catalysts in some of the aforementioned transformations.

Results and Discussion

Synthesis and Characterization of the New Ligands.

The first new ligand prepared was derived from 3-(phenyl)-4,5-dibromopyrazole. In order to have some electronic variability in the phenyl ring, we also synthesized ligands derived from 3-(*p*-tolyl)-4,5-dibromopyrazole and 3-(*p*-chlorophenyl)-4,5-dibromopyrazole. In each case, the synthesis involved reaction of the pyrazole with potassium borohydride in refluxing *p*-methylanisole. The crude salts

Scheme 2. Normal (left) and Atypical (right) Geometries for the $\text{Tp}^{\text{Br,Ph,Br}}$ Ligand



were later converted into their Tl derivatives, and crystalline material with the analytical composition $\text{Tl}[\text{Tp}^{\text{Br,Ph,Br}}]$ (**1**), $\text{Tl}[\text{Tp}^{\text{Br,p-Tol,Br}}]$ (**2**), and $\text{Tl}[\text{Tp}^{\text{Br,p-ClPh,Br}}]$ (**3**) were isolated. NMR studies revealed that, as commonly observed in these compounds, the three pyrazolyl rings were equivalent, therefore indicating that they were bonded to the boron atom with the same orientation. However, these data did not assess whether the aryl groups were bonded to the pyrazolyl ring in the 3- or in the 5-position (Scheme 2), in the so-called normal or atypical geometries, respectively.

In order to unambiguously establish the structure of these new ligands, X-ray studies were performed with single crystals of **1**, **2**, and **3**. In the three cases, these studies revealed that all of the aryl groups were in the 5-position of the ligands.¹³ The structures of **1** and **2** are shown in Figure 1. The structure of **3** was also determined, and the 5,5,5-aryl regiochemistry was also confirmed, although structural refinement could not be minimized enough (see Supporting Information).

We have also prepared two related ligands, in one case replacing the outer bromine with hydrogen (starting with 3-(*p*-chlorophenyl)-4-bromopyrazole) and in the other by a methyl group (starting with 3-phenyl-4-bromo-5-methylpyrazole). Again, NMR data were consistent with three equivalent pyrazolyl rings bonded to boron. Not unexpectedly, in both cases the structures of the derived Tl complexes, $\text{Tl}[\text{Tp}^{\text{p-ClPh,4Br}}]$ (**4**) and $\text{Tl}[\text{Tp}^{\text{Ph,Me,Br}}]$ (**5**), showed perfectly normal bonding of boron to the least-hindered nitrogen (Figure 2), with the aryl groups being in the 3-position. Therefore, it appears that the presence of bromine atoms at the central and at one outer carbon of the pyrazole is necessary to cause the “atypical” B–N bonding. We can conclude that pyrazoles of the type $\text{Hpz}^{\text{Ar,Br,Br}}$ will lead to Tp ligands with the aromatic substituent in the 5-position.

The three complexes of **1**, **2**, and **3** had a compact monomeric structure, in which the aryl groups in each case were twisted by about 70° with respect to the pyrazolyl plane and thus deviated by about 20° from orthogonality. Even so, this still provides for a large protective pocket around the B–H bond. It was also noteworthy that the B–H stretch for the three thallium complexes **1**, **2**, and **3** was rather high, in each case exceeding 2 600 cm^{-1} and thus considerably higher than that of the $\text{Tl}[\text{Tp}^{\text{Br}_3}]$ complex (2 550 cm^{-1}). These values are only surpassed by those of $\text{Tl}[\text{Tp}^x]$ ligands with a 3-trifluoromethyl substituent. The already described

- (4) (a) Rheingold, A. L.; Yap, G. P. A.; Trofimenko, S. *Inorg. Chem.* **1995**, *34*, 759. (b) Rheingold, A. L.; Haggerty, B. S.; Yap, G. P. A.; Trofimenko, S. *Inorg. Chem.* **1997**, *36*, 5097.
- (5) (a) Morilla, M. E.; Díaz-Requejo, M. M.; Belderrain, T. R.; Nicasio, M. C.; Trofimenko, S.; Pérez, P. J. *Organometallics* **2004**, *23*, 293. (b) Caballero, A.; Díaz-Requejo, M. M.; Belderrain, T. R.; Nicasio, M. C.; Trofimenko, S.; Pérez, P. J. *Organometallics* **2003**, *22*, 4145. (c) Caballero, A.; Díaz-Requejo, M. M.; Belderrain, T. R.; Nicasio, M. C.; Trofimenko, S.; Pérez, P. J. *J. Am. Chem. Soc.* **2003**, *125*, 1446.
- (6) (a) Díaz-Requejo, M. M.; Belderrain, T. R.; Nicasio, M. C.; Trofimenko, S.; Pérez, P. J. *J. Am. Chem. Soc.* **2003**, *125*, 12078. (b) Fructos, M. R.; Trofimenko, S.; Díaz-Requejo, M. M.; Pérez, P. J. *J. Am. Chem. Soc.* **2006**, *128*, 11784.
- (7) Díaz-Requejo, M. M.; Wehrmann, P.; Leatherman, M. D.; Trofimenko, S.; Mecking, S.; Brookhart, M.; Pérez, P. J. *Macromolecules* **2005**, *38*, 4966.
- (8) Morilla, M. E.; Molina, M. J.; Díaz-Requejo, M. M.; Belderrain, T. R.; Nicasio, M. C.; Trofimenko, S.; Pérez, P. J. *Organometallics* **2003**, *22*, 2914.
- (9) Caballero, A.; Díaz-Requejo, M. M.; Trofimenko, S.; Belderrain, T. R.; Pérez, P. J. *J. Org. Chem.* **2005**, *70*, 6101.
- (10) Mairena, M. A.; Díaz-Requejo, M. M.; Belderrain, T. R.; Nicasio, M. C.; Trofimenko, S.; Pérez, P. J. *Organometallics* **2004**, *23*, 253.
- (11) Urbano, J.; Belderrain, T. R.; Nicasio, M. C.; Trofimenko, S.; Díaz-Requejo, M. M.; Pérez, P. J. *Organometallics* **2005**, *25*, 1528.
- (12) Rodríguez, P.; Díaz-Requejo, M. M.; Belderrain, T. R.; Trofimenko, S.; Nicasio, M. C.; Pérez, P. J. *Organometallics* **2004**, *23*, 2162.

- (13) The abbreviations for the new ligands follow the system described in ref 1b. Since the hierarchy of substituents is established as 3-, 5-, 4-, there is no ambiguity as to the location of the substituents.

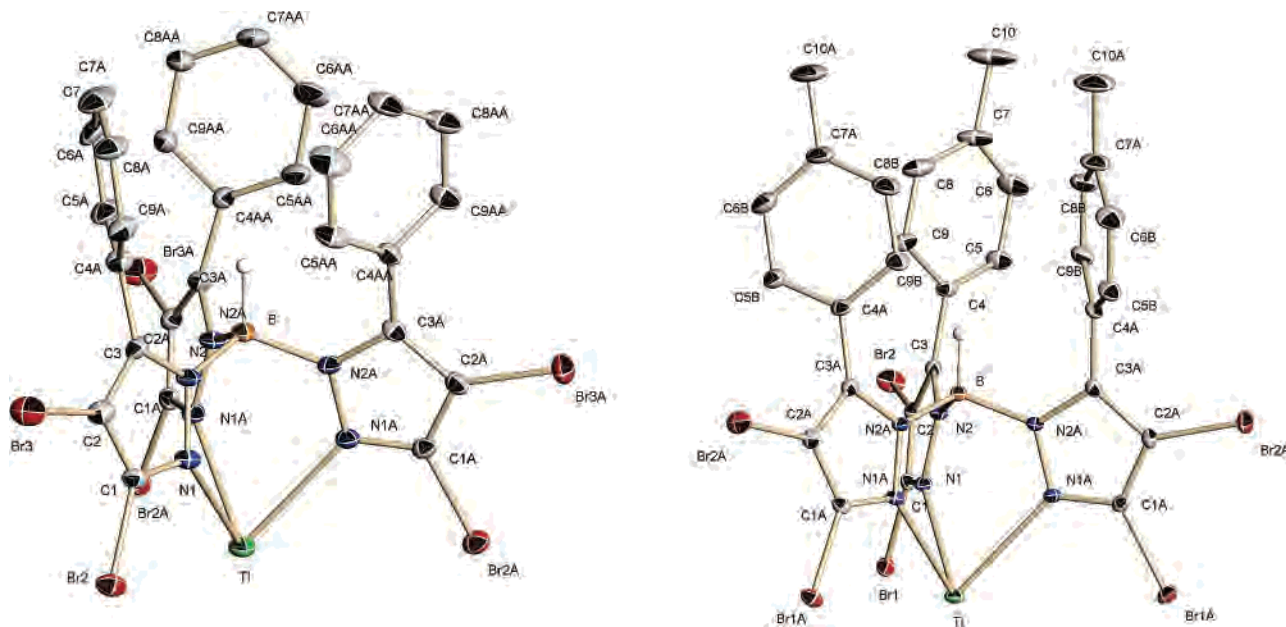


Figure 1. Molecular structures of $\text{Ti}[\text{Tp}^{\text{Br,Ph,Br}}]$ (**1**) and $\text{Ti}[\text{Tp}^{\text{Br,p-Tol,Br}}]$ (**2**), showing the atypical coordination of the pyrazolyl rings. Thermal ellipsoids are drawn at the 50% probability level. H atoms have been omitted for clarity.

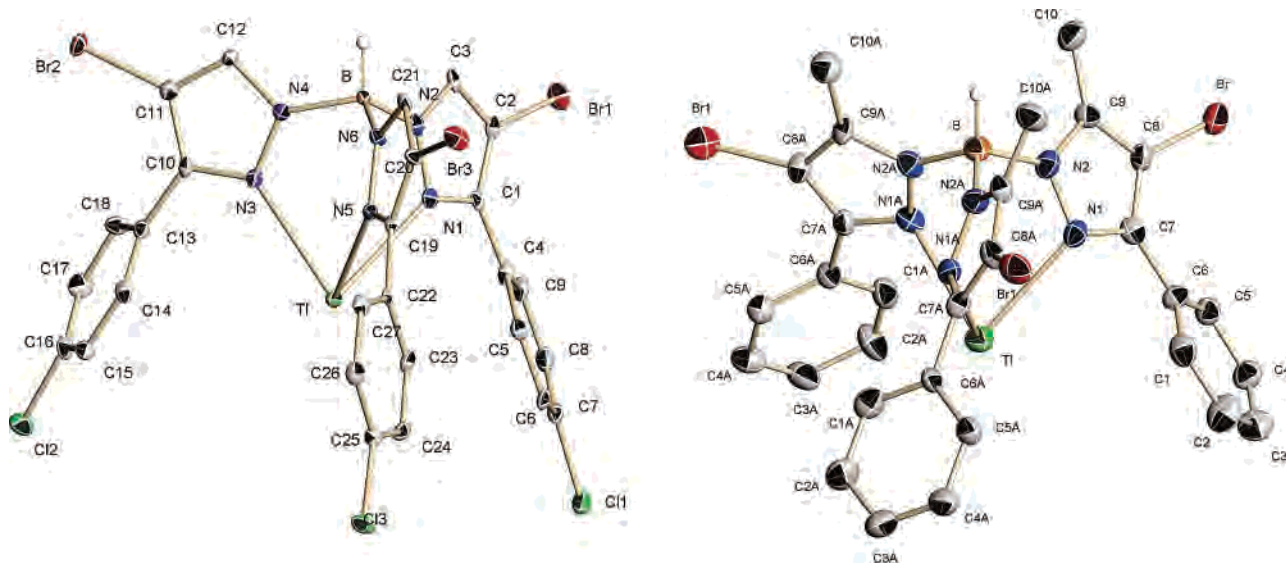


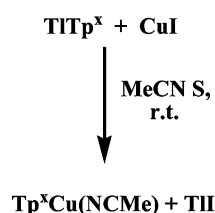
Figure 2. Molecular structures of $\text{Ti}[\text{Tp}^{\text{p-CIPh,4Br}}]$ (**4**) and $\text{Ti}[\text{Tp}^{\text{Ph,Me,Br}}]$ (**5**), showing the normal coordination of the pyrazolyl rings. Thermal ellipsoids are drawn at the 50% probability level. H atoms have been omitted for clarity.

TiTp^x ligands exhibit quite a wide range for this value, from 2 420 to 2 660 cm^{-1} .^{1,14–16} Some properties of the new $\text{Ti}[\text{Tp}^x]$ complexes, such as their B–H stretch IR values and average Ti–N distances are listed in Table 1, where they are compared with those of other reported $\text{Ti}[\text{Tp}^x]$ ligands. The Ti–N distances of the new ligands compare well within the range (2.553–2.709 Å) of previously characterized compounds. There seems to be no particular correlation between the B–H stretch and the Ti–N bond distance values.

- (14) Begtrup, M.; Boyer, G.; Cabildo, P.; Cativiela, C.; Claramunt, R. M.; Elguero, J.; García, J. I.; Toiron, C.; Vedso, P. *Magn. Reson. Chem.* **1992**, *31*, 107.
 (15) Han, R.; Ghosh, P.; Desrosiers, P. J.; Trofimenko, S.; Parkin, G. *Dalton Trans.* **1997**, 3713.
 (16) Renn, O.; Venanzi, L. M.; Marteletti, A.; Gramlich, V. *Helv. Chim. Acta* **1995**, *78*, 993.

The Tp ligands in **1**, **2**, and **3** are unique examples of Tp ligands which contain an aryl group in the 5-position and non-aryls in the 3-position. There are only two examples of Tp^x ligands with an aryl group in the 5-position, but they were derived from 3,5-diarylpzazoles where, necessarily, one substituent had to be 5-Ar by default.^{17,26} As to the reason

- (17) (a) Libertini, E.; Yoon, K.; Parkin, G. *Polyhedron* **1993**, *12*, 2539.
 (b) Rheingold, A. L.; Liable-Sands, L. M.; Incarvito, C. D.; Trofimenko, S. *J. Chem. Soc., Dalton Trans.* **2002**, 2297.
 (18) Rheingold, A. L.; Zakharov, L. N.; Trofimenko, S. *Inorg. Chem.* **2003**, *42*, 827.
 (19) Rheingold, A. L.; Incarvito, C. D.; Trofimenko, S. *J. Chem. Soc., Dalton Trans.* **2000**, 1233.
 (20) Rheingold, A. L.; Liable-Sands, L. M.; Golen, J. A.; Trofimenko, S. *Eur. J. Inorg. Chem.* **2003**, 2767.
 (21) Rheingold, A. L.; Liable-Sands, L. M.; Yap, G. P. A.; Trofimenko, S. *Chem. Commun.* **1996**, 1233.
 (22) Han, R.; Parkin, G.; Trofimenko, S. *Polyhedron* **1995**, *14*, 387.

Scheme 3. Synthesis of the Complexes $\text{Tp}^x\text{Cu}(\text{NCMe})$ 

Ligand	Complex
$\text{Tl}[\text{Tp}^{\text{Br,Ph,Br}}]$ (1)	$\text{Tp}^{\text{Br,Ph,Br}}\text{Cu}(\text{NCMe})$ (6)
$\text{Tl}[\text{Tp}^{\text{Br,p-Tol,Br}}]$ (2)	$\text{Tp}^{\text{Br,p-Tol,Br}}\text{Cu}(\text{NCMe})$ (7)
$\text{Tl}[\text{Tp}^{\text{Br,p-ClPh,Br}}]$ (3)	$\text{Tp}^{\text{Br,p-ClPh,Br}}\text{Cu}\cdot\text{CH}_2\text{Cl}_2$ (8)
$\text{Tl}[\text{Tp}^{\text{p-ClPh,4Br}}]$ (4)	$\text{Tp}^{\text{p-ClPh,4Br}}\text{Cu}(\text{NCMe})$ (9)
$\text{Tl}[\text{Tp}^{\text{Ph,Me,Br}}]$ (5)	$\text{Tp}^{\text{Ph,Me,Br}}\text{Cu}(\text{NCMe})$ (10)

Table 1. Selected $\nu(\text{B-H})$ Values (cm^{-1}) and Tl–N Bond Distances (Å) for TlTp^x Compounds

compound	B–H (cm^{-1})	Tl–N avg bond (Å)	reference
$\text{Tl}[\text{Tp}^{\text{CF}_3,\text{Tn}}]$ ^a	2660	2.620	15
$\text{Tl}[\text{Tp}^{\text{(CF}_3)_2}]$	2627	2.708	16
$\text{Tl}[\text{Tp}^{\text{Br,p-Tol,Br}}]$	2610	2.602	this work
$\text{Tl}[\text{Tp}^{\text{Br,p-ClPh,Br}}]$	2601	2.629	this work
$\text{Tl}[\text{Tp}^{\text{Br,Ph,Br}}]$	2601	2.631	this work
$\text{Tl}[\text{Tp}^{\text{(4-tBuPh)}_2}]$	2562	2.605	17a
$\text{Tl}[\text{Tp}^{\text{Br}_3}]$	2550	2.649	17b
$\text{Tl}[\text{Tp}^{\text{Bn,Me}}]$ ^a	2508	2.588	18
$\text{Tl}[\text{Tp}^{\text{cpd}}]$ ^a	2500	2.709	19
$\text{Tl}[\text{Tp}^{\text{p-ClPh,Me,Br}}]$	2491	2.600	this work
$\text{Tl}[\text{Tp}^{\text{Tol,4tBu}}]$	2472	2.563	20
$\text{Tl}[\text{Tp}^{\text{p-ClPh,4Br}}]$	2466	2.650	this work
$\text{Tl}[\text{Tp}^{\text{Bo,7tBu}}]$ ^a	2455	2.656	21
$\text{Tl}[\text{Tp}^{\text{Ant}}]$ ^a	2450	2.677	22
$\text{Tl}[\text{Tp}^{\text{p}}]$ ^b	2438	2.553	23
$\text{Tl}[\text{Tp}^{\text{Cpe}}]$ ^a	2438	2.578	24
$\text{Tl}[\text{Tp}^{\text{Bn,4Ph}}]$ ^a	2432	2.642	18
$\text{Tl}[\text{Tp}^{\text{Cbu}}]$ ^a	2428	2.562	24
$\text{Tl}[\text{Tp}^{\text{CHPh}_2}]$	2420	2.673	25

^a Tn = Thienyl; Bn = Benzyl; cpd = carboxypyrrolidido; Bo = indazol-2-yl; Ant = 9-anthryl; Cpe = cyclopentyl; Cbu = Cyclobutyl. ^b $\text{Tl}[\text{Tp}^{\text{p}}]$ = $\text{Tl}[\text{hydrotris}(1,4\text{-dihydroinden}[1,2\text{-c}]\text{pyrazol-1-yl})\text{borate}]$.

why the observed atypical B–N bonding takes place, it is most likely to be due to electronic rather than steric factors, as the boron atom prefers to be bonded to the most electron-rich nitrogen of pyrazole. Comparing the nitrogen vicinal to the aryl group with that close to the outer bromine atom, it is clear that the former offers greater electron density at the neighboring nitrogen. Additionally, complex **5** displays the expected structure, with the Me group in the 5-position, despite the larger volume of CH_3 compared with Br. This also supports the proposal that electronic effects seem to surpass the steric ones.

Synthesis and Characterization of Copper(I) Complexes of the New Ligands. As indicated above, we have been interested in the use of Tp^xCu complexes for some catalytic reactions involving carbene or nitrene transfer to organic substrates. The excellent catalytic capabilities of the complex $\text{Tp}^{\text{Br}_3}\text{Cu}(\text{NCMe})$ for those transformations led us to prepare a series of compounds with the new ligands prior to their catalytic tests. The reaction of the thallium complexes

of **1–5** with copper(I) iodide in acetonitrile induced a smooth reaction in which thallium iodide was formed and precipitated out of the reaction mixture as a yellow-greenish solid. After the mixture was stirred for 20 h, the workup yielded white crystalline materials of analytical composition $\text{Tp}^x\text{Cu}(\text{NCMe})$, with the exception of **4**, that provided $\text{Tp}^{\text{p-ClPh,4Br}}\text{Cu}\cdot\text{CH}_2\text{Cl}_2$ (**9**, Scheme 3).

From the analytical and spectroscopic data, characterization is straightforward. NMR spectra display one set of signals in each case for the three equivalent pyrazolyl rings, along with the acetonitrile resonance (see Experimental Section). Such data would support the existence of a four-coordinated environment for the copper atom, in which the three pyrazolyl rings would retain the normal or atypical geometry of the corresponding thallium salts. To prove this, we have grown single crystals of the complexes **7** and **10** and determined their solid-state structure by X-ray studies. As shown in Figure 3, both complexes maintained the relative configuration of the pyrazolyl substituents previously observed in the thallium-containing compounds. Thus, the atypical geometry shown in Figure 1 for $\text{Tl}[\text{Tp}^{\text{Br,p-Tol,Br}}]$ appears again in the molecules of **7**, the *p*-tolyl substituent being in the C5 position. The C3 position, that as mentioned above has usually been proposed as the most favorable to attach the bulkier groups, is now linked to a bromine atom. On the other hand, complex **10**, formed by the reaction of a “normal” Tp^x ligand, also displays the normal, expected geometry where the bulkier phenyl group occupies the C3 position, and the nonsubstituted, H-containing C5 position is located in the vicinity of the boron atom. Table 2 shows the main distances and angles of these two complexes. Their structures are quite similar to that reported by Tolman and co-workers for $\text{Tp}^{\text{CF}_3,\text{CH}_3}\text{Cu}(\text{NCMe})$.²⁷ A distortion from the ideal C_{3v} geometry is clearly observable on the basis of the different lengths of the Cu–N_{pyr} bonds, ranging within 2.000–2.047 Å in **7** and 2.063–2.094 Å in **10** (2.057–2.200 Å in $\text{Tp}^{\text{CF}_3,\text{CH}_3}\text{Cu}(\text{NCMe})$). The Cu–N_{NCMe} distances of 1.804 and 1.872 Å are also similar to that of Tolman’s complex of 1.875 Å. Finally, it is worth mentioning that the acetonitrile ligand falls out of the ideal axis of symmetry lying in the B–Cu direction, also inducing the observed distortion.

Catalytic Activity of the Complexes 6–10 in Carbene and Nitrene Transfer Reactions from Ethyl Diazoacetate. The interesting catalytic capabilities of the $\text{Tp}^{\text{Br}_3}\text{Cu}(\text{NCMe})$ complex toward the decomposition of ethyl diazoacetate,

(23) Rheingold, A. L.; Ostrander, R. L.; Haggerty, B. S.; Trofimenko, S. *Inorg. Chem.* **1994**, *33*, 3666.

(24) Rheingold, A. L.; Yap, G. P. A.; Zakharov, L. N.; Trofimenko, S. *Eur. J. Inorg. Chem.* **2002**, 2335.

(25) Rheingold, A. L.; Liable-Sands, L. M.; Golen, J. A.; Yap, G. P. A.; Trofimenko, S. *Dalton Trans.* **2004**, 598.

(26) Kitajima, N.; Fujisawa, K.; Fujimoto, C.; Moro-oka, Y.; Hashimoto, S.; Kitagawa, T.; Toriumi, K.; Tatsumi, K.; Nakamura, A. *J. Am. Chem. Soc.* **1992**, *114*, 1277.

(27) Schneider, J. L.; Carrier, S. M.; Ruggiero, C. E.; Young, V. G., Jr.; Tolman, W. B. *J. Am. Chem. Soc.* **1998**, *120*, 11408.

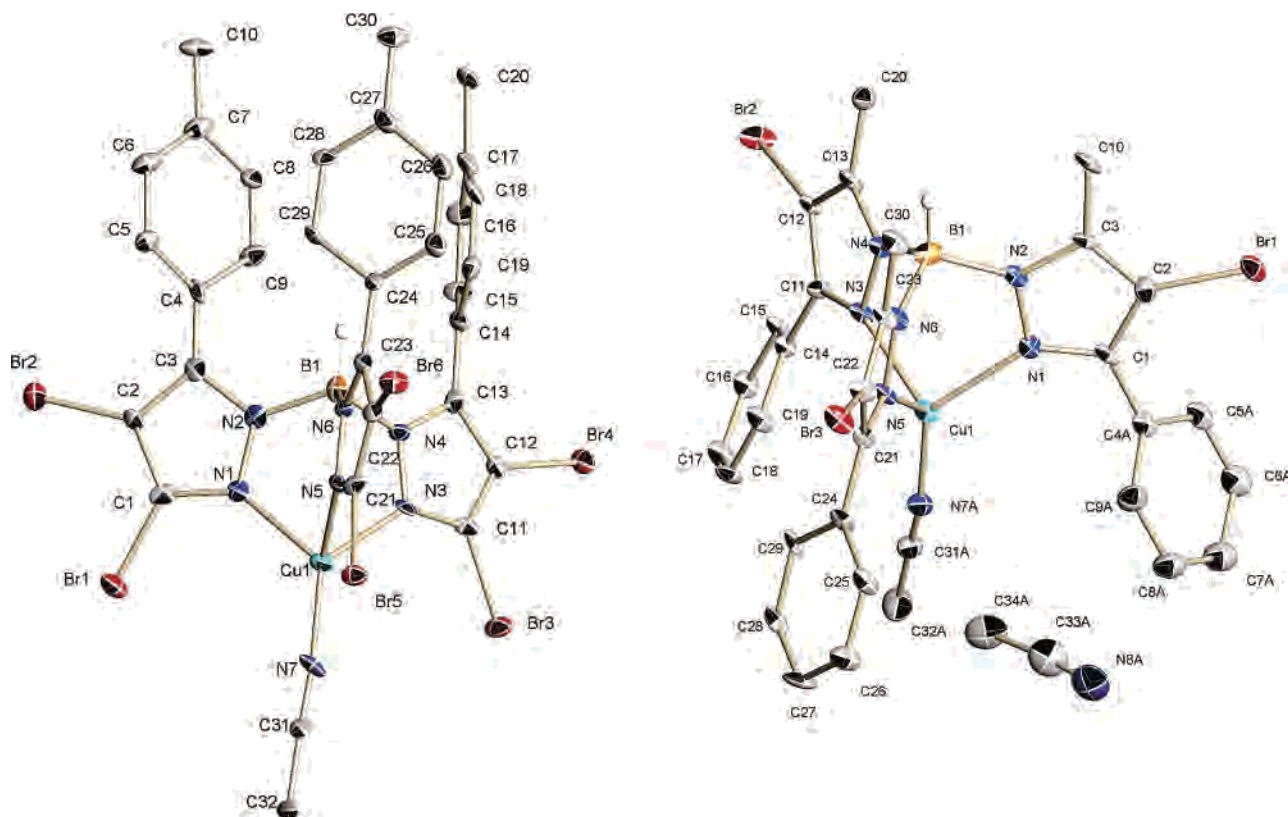


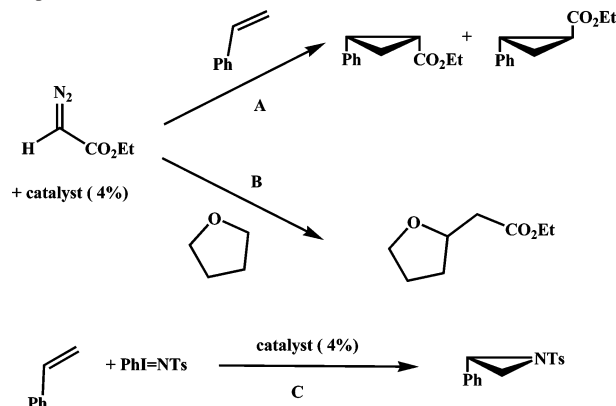
Figure 3. Molecular structures of $\text{Tp}^{\text{Br},p\text{-Tol,Br}}\text{Cu}(\text{NCMe})$ (**7**, left) and $\text{Tp}^{\text{Ph,Br,Me}}\text{Cu}(\text{NCMe})$ (**10**, right). Thermal ellipsoids are drawn at the 50% probability level. H atoms have been omitted for clarity.

Table 2. Selected Bond Distances (Å) and Bond Angles (deg) for $\text{Tp}^{\text{Br},p\text{-Tol,Br}}\text{Cu}(\text{NCMe})$ (**7**) and $\text{Tp}^{\text{Ph,Br,Me}}\text{Cu}(\text{NCMe})$ (**10**)

complex 7			
Cu(1)–N(7)	1.804(11)	N(7)–Cu(1)–N(3)	126.3(5)
Cu(1)–N(3)	2.000(10)	N(7)–Cu(1)–N(5)	124.7(4)
Cu(1)–N(5)	2.037(10)	N(3)–Cu(1)–N(5)	87.5(4)
Cu(1)–N(1)	2.047(11)	N(7)–Cu(1)–N(1)	125.7(4)
		N(3)–Cu(1)–N(1)	91.9(4)
		N(5)–Cu(1)–N(1)	89.0(4)
complex 10			
Cu(1)–N(7A)	1.872(10)	N(7A)–Cu(1)–N(5)	126.7(4)
Cu(1)–N(5)	2.063(10)	N(7A)–Cu(1)–N(3)	118.9(4)
Cu(1)–N(3)	2.075(9)	N(5)–Cu(1)–N(3)	88.6(4)
Cu(1)–N(1)	2.094(9)	N(7A)–Cu(1)–N(1)	126.2(4)
		N(5)–Cu(1)–N(1)	91.8(3)
		N(3)–Cu(1)–N(1)	94.8(3)

$\text{N}_2=\text{CHCO}_2\text{Et}$, and the subsequent transfer of the carbene moiety $:\text{CHCO}_2\text{Et}$ to saturated and unsaturated substrates have already been mentioned. The presence of bromine atoms in the Tp^x skeleton seems to favor such transfer by decreasing the electron density at the metal center. The three complexes of **6–8** display bromine atoms at C3 and C4, and therefore the catalytic pocket should be quite similar to that in $\text{Tp}^{\text{Br}_3}\text{Cu}(\text{NCMe})$. This synthetic strategy could be very useful in the preparation of new Tp^x ligands with such bromine groups at those positions and a third, distinct, bulkier group in C5 that could serve as a link to a solid support. Such linkage should not affect the catalytic pocket, since it would be located in the opposite direction. However, an obvious question arises from this reasoning, regarding the degree of influence of the substituent in the C5 position in the catalytic capabilities of these complexes.

Scheme 4. Carbene and Nitrene Transfer Reactions Catalyzed by Complexes **6–10**



With that aim in mind, we have carried out a series of experiments in which the complexes **6–10** have been employed as the catalyst in three model reactions shown in Scheme 4: (A) the cyclopropanation of styrene with ethyl diazoacetate; (B) the functionalization of tetrahydrofuran by carbene insertion into a C–H bond; and (C) the aziridination of styrene with $\text{PhI}=\text{NTs}$ as the nitrene source. The results are displayed in Table 3; all of those five complexes exhibit a catalytic activity similar to that of $\text{Tp}^{\text{Br}_3}\text{Cu}(\text{NCMe})$. The cyclopropanation of styrene has been achieved in high yield, under identical conditions (see Experimental Section), the conversion having been maintained within the range of 80–91%. The diastereoselectivity observed deserves a special comment. It is well-known²⁸ that the cis/trans ratio in this transformation is strongly influenced by the volume of the

Table 3. Carbene and Nitrene Transfer Reactions Using the Complexes **6–10** as the Catalyst^a

entry	reaction ^b	catalyst	conversion
1	A	Tp ^{Br,Ph,Br} Cu(NCMe) (6)	82 ^c (65:35) ^d
2	A	Tp ^{Br,p-Tol,Br} Cu(NCMe) (7)	84 ^c (64:36) ^d
3	A	Tp ^{Br,p-ClPh,4Br} Cu·CH ₂ Cl ₂ (8)	80 ^c (65:35) ^d
4	A	Tp ^{p-ClPh,4Br} Cu(NCMe) (9)	91 ^c (88:12) ^d
5	A	Tp ^{Ph,Me,Br} Cu(NCMe) (10)	87 ^c (85:15) ^d
6	A	Tp ^{Br₃} Cu(NCMe)	82 ^c (60:40) ^d
7	B	Tp ^{Br,Ph,Br} Cu(NCMe) (6)	70 ^e
8	B	Tp ^{Br,p-Tol,Br} Cu(NCMe) (7)	75 ^e
9	B	Tp ^{Br,p-ClPh,4Br} Cu·CH ₂ Cl ₂ (8)	82 ^e
10	B	Tp ^{p-ClPh,4Br} Cu(NCMe) (9)	82 ^e
11	B	Tp ^{Ph,Me,Br} Cu(NCMe) (10)	80 ^e
12	B	Tp ^{Br₃} Cu(NCMe)	83 ^e
13	C	Tp ^{Br,Ph,Br} Cu(NCMe) (6)	>99 ^f
14	C	Tp ^{Br,p-Tol,Br} Cu(NCMe) (7)	>99 ^f
15	C	Tp ^{Br,p-ClPh,4Br} Cu·CH ₂ Cl ₂ (8)	>99 ^f
16	C	Tp ^{p-ClPh,4Br} Cu(NCMe) (9)	>99 ^f
17	C	Tp ^{Ph,Me,Br} Cu(NCMe) (10)	>99 ^f
18	C	Tp ^{Br₃} Cu(NCMe)	>99 ^f

^a See experimental section for procedures. ^b As in Scheme 4. ^cPercentage of cyclopropanes at the end of the reaction; diethyl maleate and fumarate accounted for 100% of initial EDA. Determined by GC after total consumption of EDA. ^dCis:trans ratio. ^ePercentage of the insertion product at the end of the reaction; diethyl maleate and fumarate accounted for 100% of initial EDA. Determined by GC and NMR after total consumption of EDA. ^fDetermined by NMR after total consumption of PHI=NTs.

catalytic pocket. As inferred from data in entries 1–3, the diastereoselectivity induced by complexes **6–8** is nearly identical, evidence that the substituent at C5 does not exert any influence in the catalytic pocket. Indeed, the presence of different substituents in the aromatic ring located at that position does not seem to affect the degree of conversion. On the other hand, the use of **9** or **10** having aryl substituents at C3 clearly modifies the catalytic pocket, inducing the enhancement of the *cis*-cyclopropane. The reaction of EDA and THF in the presence of **6–10** gave the expected product in 70–82% yield, similar to the value of 83% obtained with Tp^{Br₃}Cu(NCMe). In this case, it is observable as a certain, although minor, effect of the substituent in the conversions when using **6–8** as the catalyst. The third test has been carried out with the styrene aziridination reaction; all the catalysts displayed, under the experimental conditions employed, identical catalytic capabilities, providing the aziridine in a quantitative manner.

Therefore, we believe that the above catalytic data, particularly that of complexes **6–8**, will allow the future design of new 3,4-dibromo-containing Tp^x ligands in which the C5 positions can be occupied for different groups that serve as a link to solid support. On the basis of the collected data, the catalytic activity of these supported catalysts should be quite similar to that of Tp^{Br₃}Cu(NCMe), with the added value of being an heterogeneous catalyst and the corresponding features expected from this: easy separation, catalyst recovery, and recycling.

(28) (a) Doyle, M. P.; McKervey, M. A.; Ye, T. *Modern Catalytic Methods for Organic Synthesis with Diazo Compounds*; John Wiley & Sons: New York, 1998. (b) Doyle, M. P. In *Comprehensive Organometallic Chemistry II*; Abel, E. W., Stone, F. G. A., Wilkinson, G., Eds.; Pergamon Press: Oxford, U.K., 1995; Vol 12, p 421.

Conclusion

Five new homoscorpionate ligands were prepared, three of which have an “atypical” B–N bond to the most sterically hindered pyrazole nitrogen. They contain bromine atoms on the central and outer carbons of the pyrazole ring, with all aryl substituents in the 5-position of the ligand, forming a protective pocket around the B–H bond, and have a rather high B–H stretch frequency in the IR region. The other ligands, containing no outer bromine substituents, display normal B–N bonding to the least-hindered nitrogen. The copper complexes Tp^xCu(NCMe) containing the new ligands displayed geometries in which the normal or atypical configuration of the initial ligands were maintained upon coordination to the metal center. These five complexes have been employed as the catalyst in the styrene cyclopropanation with ethyl diazoacetate, in the tetrahydrofuran functionalization with the same diazo compound, and in the styrene aziridination with PHI=NTs.

Experimental Section

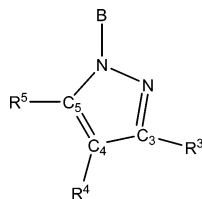
All preparations and manipulations involving copper were carried out under an oxygen-free nitrogen atmosphere using conventional Schlenk techniques or inside a drybox. All the substrates and reagents were purchased from Aldrich. Solvents were rigorously dried prior to their use in the copper chemistry. The synthesis of the starting pyrazoles followed literature procedures.²⁹ The products in the catalytic reactions were characterized as in previous work from this laboratory.^{5–12} PHI=NTs was also prepared following the already reported methods. NMR experiments were run in a Varian Mercury 400 MHz spectrometer. GC data were collected with a Varian GC-3900. IR spectra were recorded on a Perkin-Elmer 1625 FTR infrared spectrophotometer.

General Synthesis of the Pyrazoles.²⁹ The starting 3-phenylpyrazole,^{29a} 3-*p*-tolylpyrazole,^{29b} 3-*p*-chlorophenylpyrazole,²³ 3-*tert*-butylpyrazole,^{29a} and 3-phenyl-5-methylpyrazole,^{29c} were prepared by the literature methods. The dibromination of 3-substituted pyrazoles was achieved in the following manner. The appropriate pyrazole was dissolved in methanol, containing 3 equiv of sodium hydroxide. Two equivalents of bromine was slowly added dropwise to this solution. After completion of the addition, the solution was stirred for another hour and was then slowly added to a large amount of water, containing excess hydrochloric acid. The precipitated product was filtered off and was partially air-dried. It was then taken up in ethyl acetate, which allowed for the separation of the remaining aqueous layer. The organic phase was passed through a short layer of alumina, and the eluate was evaporated to dryness to yield the desired pyrazole with analytical purity.^{29d}

Synthesis of TITp^x. General Procedure. A mixture of the appropriate pyrazole and KBH₄, in a 3.5:1 mole ratio, was stirred and refluxed in 4-methylanisole, with monitoring of hydrogen evolution with a bubbler. When no more hydrogen was evolved (24–30 h), the solvent was removed under vacuum, and the residue

(29) (a) Trofimenko, S.; Calabrese, J. C.; Thompson, J. S. *Inorg. Chem.* **1987**, *26*, 1507. (b) Trofimenko, S.; Calabrese, J. C.; Kochi, J. K.; Wolowicz, S.; Hulsbergen, F. B.; Reedijk, J. *Inorg. Chem.* **1992**, *31*, 3943. (c) Lopez, C.; Sanz, D.; Claramunt, R. M.; Trofimenko, S.; Elguero, J. *J. Organomet. Chem.* **1995**, *503*, 265. (d) The detailed synthesis as well as analytical, spectroscopic, and crystallographic data of the new pyrazoles are being published separately. Claramunt, R. M.; García, M. A.; Santa-Maria, M. A.; Elguero, J.; Jove, F.; Gap, G. P. A.; Trofimenko, S. Manuscript in preparation.

was dissolved in THF. The slightly turbid solution was filtered through celite and slowly poured into an aqueous solution of 1.1 equiv (based on borohydride) of thallium nitrate or sulfate. Chloroform was added, and the mixture was vigorously stirred for 3 h. At this point there was either a clear two-layer system or two layers with a white precipitate at the bottom, which was the Tl salt of the ligand. After filtration, any solid separated was washed with successive small amounts of chloroform and acetone and methanol, and it was then air-dried. The bottom phase of the two-phase filtrate was separated and evaporated to dryness. The residue was stirred with a 1:1 mixture of acetone and methanol (in which the pyrazoles are quite soluble whereas the Tl salt of the ligand is only sparingly soluble), the slurry was filtered, and the residue was washed with the acetone–methanol mixture. The solid was air-dried and combined with the original precipitate. Yields ranged from 60 to 70%. The mother liquors were hydrolyzed in aqueous acetic acid to recover the starting pyrazole.



Tl[Tp^{Br,Ph,Br}] (1). White solid, sinters from 252 °C, mp ~270 °C. IR: BH 2 600 cm⁻¹. ¹H NMR (400 MHz, tol-*d*₈): δ (ppm) 6.88 (t, 3H), 6.66 (t, 6H), 6.55 (d, 6H), ³J_{H-H} = 8 Hz. ¹³C{¹H} NMR (100 MHz, Tol-*d*₈): δ (ppm) 148.9 (C₅), 130.4, 128.3 (C–H phenyl), 97.4 (C₄). Solvent obscured the other resonances. Anal. Calcd for C₂₇H₁₆BBR₆N₆Tl: C, 29.0; H, 1.4; N, 7.5. Found: C, 28.7; H, 1.6; N, 7.3.

Tl[Tp^{Br,p-Tol,Br}] (2). White solid, mp 282–285 °C. IR: BH 2 610 cm⁻¹. ¹H NMR (400 MHz, CDCl₃): δ (ppm) 6.76, 6.67, (AA'XX' spin system, J_{app} = 8 Hz, H, aryl), 2.36 (Me). ¹³C{¹H} NMR (100 MHz, CDCl₃): δ (ppm) 148.9 (C₅), 138.4 (C_{aryl}–Me), 130.3, 128.5 (C–H aryl), 128.1 (C₃), 126.6 (C_{ipso}), 97.0 (C₄), 21.5 (Me). Anal. Calcd for C₃₀H₂₂BBR₆N₆Tl: C, 31.0; H, 1.9; N, 7.2. Found: C, 31.1; H, 2.1; N, 7.1.

Tl[Tp^{Br,p-ClPh,Br}] (3). White solid; mp unchanged up to 310 °C. IR: BH 2 601 cm⁻¹. ¹H NMR (400 MHz, CDCl₃): δ (ppm) 7.05, 6.68 (AA'XX' spin system, J_{app} = 8 Hz, H, aryl). ¹³C{¹H} NMR (100 MHz, CDCl₃): δ (ppm) 147.6 (C₅), 138.1 (C_{aryl}–Cl), 135.7 (C_{aryl}–C₅), 131.7 (C_{aryl}–H), 128.3 (C_{aryl}–H), 97.5 (C₄). The resonance of C₃ is obscured by those of C_{aryl}. Anal. Calcd for C₂₇H₁₃BBR₆Cl₃N₆Tl: C, 26.5; H, 1.1; N, 6.9. Found: C, 26.2; H, 1.3; N, 6.6.

Tl[Tp^{p-ClPh,4Br}] (4). White solid, mp 281–283 °C. IR: BH 2 466 cm⁻¹. ¹H NMR (400 MHz, CDCl₃): δ (ppm) 7.81 (H, R⁵), 7.53, 6.44 (AA'XX' spin system, J_{app} = 8 Hz, H, aryl). ¹³C{¹H} NMR (100 MHz, CDCl₃): δ (ppm) 150.1 (C₃), 138.2 (C_{ipso} aryl), 134.9 (C–H pyrazol), 130.1, 129.3 (C–H, aryl), 93.8 (C₄). Anal. Calcd for C₂₇H₁₆BBR₃Cl₃N₆Tl: C, 32.9; H, 1.6; N, 8.5. Found: C, 33.0; H, 1.8; N, 8.3.

Tl[Tp^{Ph,Me,Br}] (5). White solid, mp 244–246 °C. IR: BH 2 491 cm⁻¹. ¹H NMR (400 MHz, CDCl₃): δ (ppm) 7.20 (br d, 2 H phenyl), 6.98 (m, 3H phenyl), 2.16 (s, Me). ¹³C{¹H} NMR (100 MHz, CDCl₃): δ (ppm) 149.7 (C₅), 144.2 (C₅), 132.3, 128.8, 128.6 (C–H phenyl), 94.5 (C₄), 12.4 (Me). Anal. Calcd for C₃₀H₂₈BBR₃N₆Tl: C, 38.8; H, 3.0; N, 9.1. Found: C, 38.6; H, 3.4; N, 9.0.

Synthesis of the Complexes Tp^xCu(NCMe). Copper iodide (95 mg, 0.5 mmol) was added to a solution of TlTp^x (0.5 mmol) in acetonitrile, and the mixture was stirred at room temperature for

20 h. After that time, the resulting suspension was filtered through celite, and the colorless solution was concentrated under vacuum and cooled at –20 °C to give white microcrystalline materials of composition Tp^xCu(NCMe) in 70–90% yield. The Tl[Tp^{p-Cl-Ph,4-Br}]-containing complex was synthesized in methylene chloride, leading to the isolation of a CH₂Cl₂-containing compound.

Tp^{Br,Ph,Br}Cu(NCMe) (6). ¹H NMR (400 MHz, CD₂Cl₂): δ (ppm) 7.30 (t, 3H), 6.98 (t, 6H), 6.82 (d, 6H), J_{H-H} = 12 Hz, 2.04 (MeCN). ¹³C{¹H} NMR (100 MHz, CD₂Cl₂): δ (ppm) 147.8 (C₅), 130.3, 129.3, 128.8, 128.6, 127.9, 96.4 (C₄). IR (Nujol mull): ν(B–H) = 2 626 cm⁻¹. Anal. Calcd for C₂₉H₁₉N₇Br₆BCu: C, 34.2; H, 1.9; N, 9.6. Found: C, 34.0; H, 1.9; N, 10.26.

Tp^{Br,p-Tol,Br}Cu(NCMe) (7). ¹H NMR (400 MHz, CD₂Cl₂): δ (ppm) 6.75, 6.69 (AA'XX' spin system, J_{app} = 8 Hz, H, aryl), 2.37 (Me), 2.04 (MeCN). ¹³C{¹H} NMR (100 MHz, CD₂Cl₂): δ (ppm) 147.9 (C₅), 138.7 (C_{aryl}–Me), 130.2, 128.5 (C_{aryl}–H), 128.3 (C₃), 126.4 (C_{ipso}), 96.02 (C₄), 21.2 (Me). IR (Nujol mull): ν(B–H) = 2 626 cm⁻¹. Anal. Calcd for C₃₂H₂₅N₇Br₆BCu: C, 36.2; H, 2.4; N, 9.2. Found: C, 35.5; H, 2.3; N, 9.5.

Tp^{Br,p-Cl-Ph,Br}Cu(NCMe) (8). ¹H NMR (400 MHz, CD₂Cl₂): δ (ppm) 7.06, 6.76 (AA'XX' spin system, J_{app} = 8 Hz, H, aryl), 2.05 (MeCN). ¹³C{¹H} NMR (100 MHz, CD₂Cl₂): δ (ppm) 146.5 (C₅), 135.4 (C_{aryl}–Cl), 131.7 (C_{aryl}–C₅), 128.8 (C_{aryl}–H), 128.3 (C_{aryl}–H), 127.9 (C_{aryl}–C₃), 96.6 (C₄). IR (Nujol mull): ν(B–H) = 2 633 cm⁻¹. Anal. Calcd for C₂₉H₁₆N₇Br₆Cl₃BCu: C, 31.0; H, 1.4; N, 8.7. Found: C, 30.5; H, 1.4; N, 9.1.

Tp^{p-Cl-Ph,4-Br}Cu·CH₂Cl₂ (9). ¹H NMR (400 MHz, CD₂Cl₂): δ (ppm) 8.05 (H, R⁵), 6.8, 6.54 (AA'XX' spin system, J_{app} = 8 Hz, H, aryl). ¹³C{¹H} NMR (100 MHz, CDCl₃): δ (ppm) 150.8 (C₃), 140.6 (C_{ipso}aryl), 134.5 (C–H pyrazol), 130.6, 129.7 (C–H, aryl), 94.3 (C₄). IR (Nujol mull): ν(B–H) = 2 453 cm⁻¹. Anal. Calcd for C₂₈H₁₈N₆Br₃Cl₃BCu: C, 36.1; H, 1.9; N, 9.0. Found: C, 37.2; H, 1.9; N, 9.3.

Tp^{Ph,Me,Br}Cu(NCMe) (10). ¹H NMR (400 MHz, CDCl₃): δ (ppm) 7.75 (br d, 2H phenyl), 7.39 (m, 3H, phenyl), 2.52 (s, Me), 2.04 (MeCN). ¹³C{¹H} NMR (100 MHz, CDCl₃): δ (ppm) 148.4 (C₅), 143.3 (C₃), 132.3, 129.3, 128.6, 127.8 (C–H phenyl), 93.2 (C₄), 11.9 (Me). IR (Nujol mull): ν(B–H) = 2 543 cm⁻¹. Anal. Calcd for C₃₂H₂₈N₇Br₃BCu: C, 46.6; H, 3.4; N, 11.9. Found: C, 46.5; H, 3.3; N, 12.5.

Catalytic Experiments: (a) Styrene cyclopropanation. To a solution of 0.02 mmol of the copper complexes **6–10** in 10 mL of methylene chloride, 125 equiv of styrene (2.5 mmol) and 25 equiv of ethyl diazoacetate (0.5 mmol) were added in one portion. The mixture was stirred at room temperature for 1 h and then analyzed by GC. (b) Tetrahydrofuran functionalization. The copper complexes **6–10** (0.02 mmol) were dissolved in THF (5 mL), and 50 equiv of ethyl diazoacetate (1 mmol) was added in one portion. No EDA was detected by GC after 1 h of stirring. Volatiles were removed under vacuum, and the residue was investigated by GC and NMR. (c) Styrene aziridination. The copper complex (0.02 mmol) and styrene (125 equiv, 2.5 mmol) were dissolved in methylene chloride (10 mL). Molecular sieves were placed into the reaction flask to avoid the presence of adventitious water. PhI=NTs (0.5 mmol) was then added in one portion, and the mixture was stirred until no solid PhI=NTs was observed. The mixture was filtered off, the volatiles were removed under vacuum, and the residue was investigated by NMR, showing the exclusive presence of the expected aziridine in quantitative yield.

X-ray Crystallography. Crystals of **1–5** were selected and mounted on glass fibers with viscous oil and cooled to the data collection temperature. Diffraction data were collected on a Bruker-AXS APEX diffractometer. All data sets were treated with

SADABS³⁰ absorption corrections. No symmetry higher than triclinic was observed in the diffraction data for **4**. The unit-cell parameters, patterns of absences, and equivalent reflections in the diffraction data were consistent for lower-symmetry trigonal Laue class-3, space groups *P*3 and *P*-3 for **1** and **2**, and *R*3 and *R*-3 for **5**. The structural solutions in the centrosymmetric space group option yielded chemically reasonable and computationally stable results of refinement for **4** (*P*-1), **1** (*P*-3), and **2** (*P*-3). The absence of a molecular -3 axis and occupancy of three in **5** suggested *R*3 for **5**. The Flack parameter refined to nil indicating that the true hand of the data in **5** had been correctly determined. The data sets of **1** and **2** were treated with the Squeeze filter of PLATON,³¹ and void space analyses are consistent with disordered, cocrystallized solvent molecules, one chloroform molecule/cell in **1** and four ethanol molecules/cell in **2**. The compound molecules in **1**, **2**, and **5** are located at 3-fold rotation axes. Phenyl groups in **1** were treated as idealized, flat, hexagonal, rigid groups. All non-hydrogen atoms were refined with anisotropic displacement parameters. Hydrogen atoms on the boron atoms were located from the difference map and were treated with a riding model with *U* constrained to 0.20*U*_{eq} of the boron atom. All other hydrogen atoms were treated as idealized contributions. All software and sources of the scattering factors are contained in various versions of the SHELXTL program library.³²

A representative single crystal of suitable size of **7** or **10** was coated with perfluoropolyether oil (FOMBLIN 140/13, Aldrich) and mounted, in the cold N₂ stream of the Kryoflex attachment of a Bruker-Nonius Kryo-Flex low-temperature device cooled at 100 K, on a glass fiber and attached to the goniometer head on a Bruker-Nonius X8Apex-II CCD diffractometer using a graphite monochromator with $\lambda(\text{Mo K}\alpha_1) = 0.71073 \text{ \AA}$. Data collection was performed by using ω and φ scans with a width of 0.30 and 20 s

(30) Sheldrick, G. M. *SADABS*; Bruker AXS, Inc.: Madison, WI, 1999.

(31) Spek, A. L. *J. Appl. Crystallogr.* **2003**, *36*, 7–13.

(32) *SHELXTL 6.14*; Bruker AXS, Inc.: Madison, WI, 2000–2003.

(in the range $4.50^\circ < 2\theta < 54.44^\circ$) of exposure times with a detector distance of 37.5 mm. The raw data were reduced to *F*² using the SAINT³³ software, and global refinements of unit cell parameters employing 6972–7185 reflections chosen from the full data sets were performed. Multiple measurements of equivalent reflections provided the basis for empirical absorption corrections as well as corrections for Lorentz polarization effects and any crystal deterioration during the data collection (multiscan method applied by SADABS).³⁰ The structure was solved by direct methods (SIR-2002)³⁴ and refined against all *F*² data by full-matrix least-squares procedures minimizing $w(F_o^2 - F_c^2)^2$ using the SHELXTL-6.12 package.³² All the non-hydrogen atoms were refined with anisotropic displacement parameters. The hydrogen atoms were included from calculated positions (C–H = 0.95 Å (aromatic rings) or 0.98 Å (methyl groups)) and refined as riding contributions with isotropic displacement parameters 1.2 (aromatic rings) or 1.5 (methyl groups) times those of their respective attached carbon atoms. Weighted *R* factors (*R*_w) and all goodness-of-fit *S* values are based on *F*²; conventional *R* factors (*R*₁) are based on *F*.

Acknowledgment. Financial support of this work from MEC (CTQ2005-00324/BQU) is acknowledged. The Universidad de Huelva (Plan Propio de Investigación), Junta de Andalucía (JU), and the Ramon y Cajal Program (MMDR) are also acknowledged.

Supporting Information Available: X-ray crystallographic data in CIF format. This material is available free of charge via the Internet at <http://pubs.acs.org>.

IC061714Z

(33) *SAINT 6.02*; Bruker AXS, Inc.: Madison, WI, 1997–1999.

(34) Burla, M. C.; Camalli, M.; Carrozzini, B.; Cascarano, G. L.; Giacovazzo, C.; Polidori, G.; Spagna, R. *SIR2002*, the program *J. Appl. Crystallogr.* **2003**, *36*, 1103.